This article has been accepted for publication in a future issue of this journal, but has not been fully edited. Content may change prior to final publication. Citation information: DOI 10.1109/TNS.2016.2632064, IEEE Transactions on Nuclear Science

Emerging New Pseudobinary and Ternary Halides as Scintillators for Radiation Detection

Byungkyun Kang†, Qingguo Feng†, C. Summers, C. M. Fang, Rajendra Adhikari, and Koushik Biswas

***Abstract*— Recently there has been a discernible shift from simple binary halide scintillators (e.g., NaI, CsI) toward host compounds that are structurally and electronically more complex. Besides SrI_2 and $LaBr_3$, several pseudobinary, ternary and quaternary halides have emerged as promising scintillators for radiation detection. Here, we survey our recent first-principles based computational studies of different hosts belonging to a class of mixed halides or distinct stoichiometric compounds. The mixed halides comprise of simple binary end members, NaI or CsI, that are known scintillators. The ternary compounds belong to a family of iodides of the type AB_2I_5 or ABI_3, where the A and B cations are alkali and alkaline-earth metals, respectively. These are usually activated by Eu^{2+}. We will consider Eu-dopant behavior in these compounds before delving into a set of ns^2 containing ternaries. They are analogous to the AB_2I_5 group of materials, except that the ns^2 ion is part of the crystal framework, replacing the alkali "A" ion, e.g., $InBa_2I_5$ or $TlBa_2I_5$. Interestingly, we predict Eu^{2+} activation will be rendered ineffective in these ns^2 compounds, caused by changes in the valence and conduction band edges. However, the possibility of fast electron capture at ns^2 sites and the prospect of self-activated scintillation could be interesting for detector applications.**

***Index Terms*—scintillator, radiation detector, ternary halides, mixed halides.**

I. Introduction

WITHIN the past decade or so there has been a renewed emphasis on finding improved scintillators that can meet the current challenges of identifying radioactive sources in a diverse setting. The main driving principle behind this search is to have low cost detectors appropriate for nuclear nonproliferation applications, having moderate to high light yield, acceptable time response and excellent energy resolution ideally in the 2-3% range at 662 keV. These pre-conditions led to a shift in focus from simple binary halide scintillators (e.g., NaI, CsI) toward compounds that are structurally and electronically more complex. It will be noticed that many of the potential scintillators that approach the near-theoretical light yield limit and exhibit the best gamma resolution depart from the simple crystalline basis of NaI or CsI and may be informally classified as being "complex" metal halide crystals. Besides SrI_2 [1] and $LaBr_3$ [2], several ternary and quaternary halides have emerged as part of this group of promising scintillators [3]-[11]. It is an interesting development: on one hand there are often inherent difficulties associated with growing these crystals, on the other they allow more flexibility and configurational degrees of freedom to optimize properties.

First-principles based computational methods is a powerful tool in screening and characterizing these new materials. In addition to ground state properties and material thermodynamics, improved variants of density functional theory (DFT) [12] provide detailed insight into the opto-electronic processes, formation of native defects, behaviors of dopants, polarons, and excitons – without relying on empirical inputs. We should note that unambiguous interpretation of results obtained from DFT based methods needs careful attention to its limitations. Recent advances made in the development of hybrid functionals [13],[14] and implementation of many-body perturbation theory [15] often drastically improve the accuracy of calculations, albeit at considerable (if not prohibitive) computational cost. Theory based predictive approaches can go hand-in-hand with experiment in the effective design and development of functional scintillators.

Taking cue from experimental and phenomenological evidence, we have recently focused our computational search for improved halide scintillators in two main directions. First, is a group of mixed crystals obtained from solid solutions of simple binary end members. This choice falls within the realm of easily growable binary compounds that are already known scintillators and the possibility that their solid solutions may favorably impact electronic and vibrational properties. The second avenue for research comprise of a family of ternary compounds that depart from the class of simple cubic or rocksalt structures having favorable electronic properties that comes at the cost of crystalline complexity. This paper intends to provide a sampling of those efforts where we have performed density functional based calculations in order to characterize different ternary halides. Although these are predicted properties, connections with experimental observations will be attempted whenever possible.

II. Computational Method

All calculations are based on DFT as implemented in the plane wave code, Vienna Ab-initio Simulation Package (VASP) [16], [17]. The exchange-correlation functionals as parameterized by Perdew-Burke-Ernzerhof (PBE) within the

By. Kang, Q. Feng, C. Summers, C. M. Fang, R. Adhikari, and K. Biswas are with the Department of Chemistry and Physics, Arkansas State University, State University, AR 72467, USA (e-mail: kbiswas@astate.edu).
† B.K. and Q. F. contributed equally to this work.

This article has been accepted for publication in a future issue of this journal, but has not been fully edited. Content may change prior to final publication. Citation information: DOI 10.1109/TNS.2016.2632064, IEEE Transactions on Nuclear Science

generalized gradient approximation (GGA) have been used [18]. Electron-ion interactions are described by projector augmented wave potentials [19], [20]. Even though DFT is an exact ground state theory, local and semilocal approximations to the exchange and correlation energy introduce a well-known "band gap problem", where calculated gap is smaller than the experimental values of many semiconductors and insulators. These approximations suffer from self-interaction errors which lead to the band gap problem and it may affect the properties of defects and impurities and localization behavior of charge carriers. Appropriate use of hybrid functionals that use a fraction of the Hartree-Fock exact exchange can remedy this problem, giving more accurate estimations of band gap. We have used hybrid PBE0 functional [14] on an as-needed basis in order to provide a comprehensive outlook of the compounds under study. For all the calculations the valence wave functions are expanded on a plane-wave basis with cutoff energies ranging between 250-300 eV for the different sets of compounds. The mixed halides are simulated using 16-atom special quasi-random structures (SQS) [21], [22]. A Γ-centered k-mesh with varying k-points (depending upon the shape of the generated SQS and other unit cells) has been used for sampling the Brillouin zone and all structures are relaxed until the force components are less than 0.01 eV/Å. Electronic band structure and phonon density of states of the mixed halides are calculated using fully relaxed 16-atom cells. As there are 3N phonon modes the lattice vibration calculations are computationally demanding for large supercells. For accurately calculating phonon frequencies we have implemented a mixed space approach as suggested in [23]. Electronic structure calculations including spin-orbit coupling (SOC) were done within the PBE method (PBE-SOC). In case of the AB_2I_5, ABI_3 and ns^2-compounds we have investigated Eu^{2+} doping by using 2×2×1 or 2×2×2 supercells. We adopted the PBE+U approach [24] with U_{eff} = 2.5 eV to describe the localized Eu 4*f* levels. Similar U_{eff} parameter has been previously used [25] to appropriately model the localization of the Eu 4*f* states.

III. Results and Discussion

A. Solid solutions or mixed binaries

Gektin et al., [26] pointed out that there was evidence of higher light yield among mixed crystals and this empirical observation was independent of crystal type and even persisted among halide, oxide and sulfate scintillators. They even remarked that the improved scintillation light yield could be achieved near the 50% composition of mixed crystals relative to the pure end members. One example of this behavior is the mixed halide BaBrI developed independently by Bourret-Courchense et al., [11] which has reported light yield and energy resolution superior to those of the binary end members, $BaBr_2$ and BaI_2. All these developments led us to our own investigations of representative systems of mixed alkali halides, viz., NaI_xBr_{1-x} that has mixing in the anion sublattice and $Na_xK_{1-x}I$ that has disorder in the cation sublattice. We found that the complexities introduced by the non-identical atoms in terms of low hot electron group velocity were

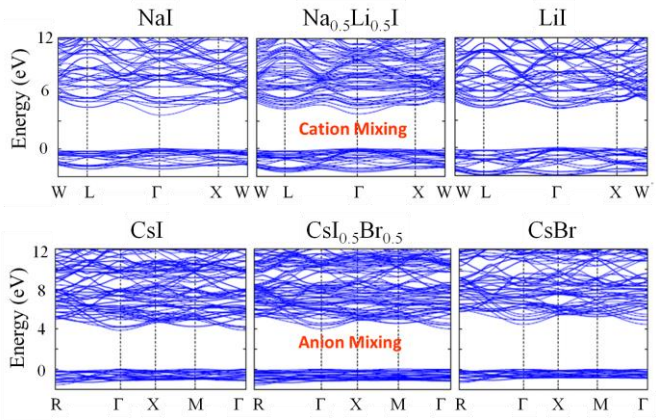

Fig. 1. Calculated electronic band structures of the parent and mixed halides. The zero of energy is set at the top of the valence bands. Band gaps are underestimated.

TABLE I
ELECTRON BAND MASS m_b OF DIFFERENT BINARIES AND ALLOYS

Concentration	$Li_xNa_{1-x}I$	$NaBr_xI_{1-x}$	$K_xNa_{1-x}I$	$CsBr_xI_{1-x}$
0.0	0.268	0.268	0.268	0.280
0.125	0.274	0.276	0.276	0.296
0.5	0.289	0.298	0.312	0.308
1.0	0.333	0.317	0.33(0.4)[a]	0.305

[a]Experimental electron band mass[28]

indicative of better performance at least in case of the mixed cation compound, $Na_{0.5}K_{0.5}I$ [27].

Following those previous works [27], we report our recent work on $Na_{1-x}Li_xI$ (mixed cation) and $CsI_{1-x}Br_x$ (mixed anion). Our choice of systems for mixed crystals is based on two classic scintillators, NaI and CsI. To mimic the alloying we simulated 16-atom SQS cells for the intermediate compositions of the mixed hosts. Fig. 1 shows the familiar tangle of electronic bands of the parent and mixed halides. Note that in order to remain consistent all band structures are generated with 16 atom cells. Mixing introduces heavier and flatter upper conduction bands without affecting the conduction band minimum (CBM). As such, the thermalized electron will retain its free carrier-like property at band edge as evidenced from our calculated band mass shown in Table I. The electron effective mass (m_b) are calculated within the parabolic band approximation using,

$$\frac{1}{m_b} = \frac{1}{\hbar^2}\frac{\partial^2 E}{\partial k^2}. \quad (1)$$

The top of the valence bands in these halides remain characteristically narrow and dispersion-less, which will ensure prompt self-trapping of holes (STH) after excitation. Retaining the dispersive nature of CBM in mixed halides, for example in $Na_{0.5}Li_{0.5}I$ and $CsI_{0.5}Br_{0.5}$ is significant (Fig. 1, Table I). The thermalized electrons will not self-trap, that will aid their radiative recombination with the STHs. On the other hand, the denser tangle of upper conduction bands (i.e., heavier) will at least hinder the diffusion of hot electrons and limit nonradiative capture at localized defects. We may contrast this behavior with another well-known scintillator $Cs_2LiYCl_6:Ce^{3+}$ (CLYC). In CLYC, the Y-*d* states form a narrow CBM [29] which promotes

This article has been accepted for publication in a future issue of this journal, but has not been fully edited. Content may change prior to final publication. Citation information: DOI 10.1109/TNS.2016.2632064, IEEE Transactions on Nuclear Science

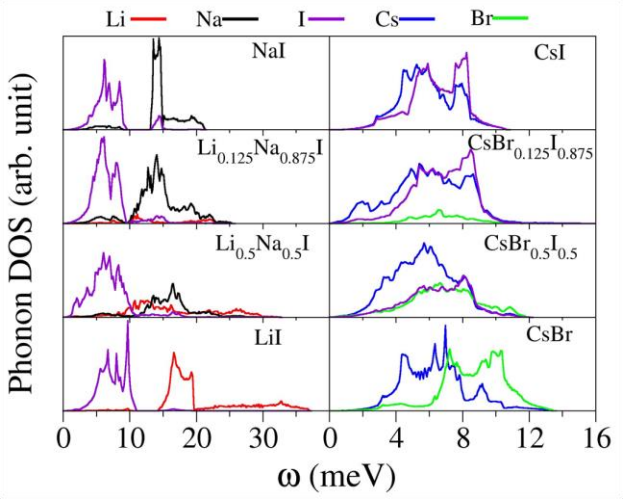

Fig. 2. Evolution of the phonon density of states for $Li_xNa_{1-x}I$ system (left panel) and $CsBr_xI_{1-x}$ system (right panel) with changing composition of the mixture.

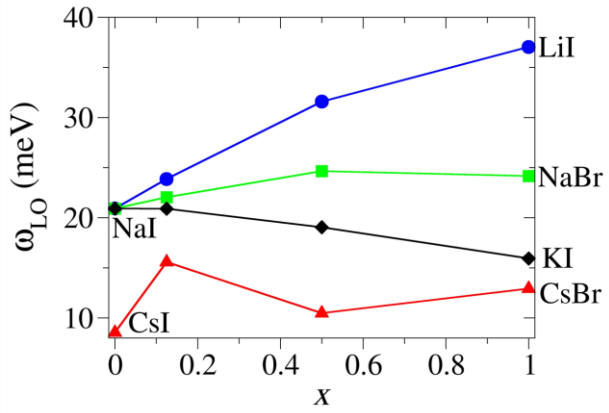

Fig. 3. Comparison of LO phonon energies at Γ-point of four mixed halides as a function of concentration. Square and triangle symbols represent the anion mixing while circle and diamond represent cation mixing.

the self-trapping of electrons. The electron polarons combine with a STH forming a self-trapped exciton (STE). Consequently, the light yield is affected by the inefficient diffusion of the STE to a Ce^{3+} luminescent center in CLYC, resulting in a relatively low ~20 000 photons/MeV output and a slow decay time of several μs [4]-[9]. Unlike CLYC, the binary halides have higher light yield and smaller decay times – a property that should also be retained in the mixed halides. Mixing in the cation/anion sublattice may have additional advantages in terms of band gap engineering and possibility of more efficient activator doping.

The coupling between longitudinal optical (LO) phonons and electrons play an important role during the thermalization of hot carriers. It is one of the many crucial factors determining scintillator performance. Therefore, it is important to understand the evolution of the phonon spectrum upon alloying. We have calculated the phonon spectra of binary alkali halides and their mixtures. Fig. 2 shows the phonon density of states (DOS) of the two mixed halide systems. In case of the binary NaI and LiI the phonon DOS curves are well separated into two parts: the lower part is composed of acoustic contributions from the heavy I anions, meanwhile, the lighter Li or Na cations contribute to the higher energy part of the spectra. For the mixed compositions, the acoustic modes dominated by I remain relatively unchanged while the higher energy optical modes shift according to Li/Na alloying.

Another example is the $CsI_{1-x}Br_x$ system, where contributions from Cs and I are in the same energy range due to similarity in their masses, and therefore, we find overlapping peaks in the phonon DOS. With increasing concentration, the peaks become broader and shift towards higher energy, mainly due to incorporation of the light Br atom.

The precise changes in the vibrational modes are more complicated in the mixed crystals due to additional branches in the phonon spectrum caused by alloying. However, it may be argued that those additional optical branches and the continuum of low frequency LO phonons available in the mixed halides (Fig. 2) will slow down electron thermalization rate. The hot carriers remain free for an extended time (order of ps), which inhibits dipole-dipole quenching. This in conjunction with the heavy upper conduction bands described earlier will limit hot electron diffusion and may favorably impact radiative recombination and light yield in mixed crystals.

Fig. 3 shows the calculated highest energy LO mode at Γ-point of four mixed compounds as a function of concentration. The LO frequency varies almost linearly with composition except in $CsI_{1-x}Br_x$, where there is a clear spike in the frequency at 12.5% Br concentration. This anomalous result takes on added significance when we consider Gektin et al's observation of CsI-Br mixed crystals showing accelerated decay kinetics and increased light yield especially around 10% Br compared to pure CsI [26]. Further investigations will be necessary to clarify this behavior. However, it is evident that the phonon modes can be effectively tuned by controlling the concentration, which in turn could help optimize electron-phonon coupling and hot carrier thermalization.

B. Monoclinic iodides, AB_2I_5 family (A=alkali, B=alkali-earth metal)

Another sub-topic in the area of complex halides are a family of iodides belonging to the formula type AB_2I_5 where A = alkali and B = alkali-earth metal. Although these materials have a monoclinic crystal structure, [30], [31] members of this family e.g., $CsBa_2I_5$ and KSr_2I_5 have already shown promising characteristics. When doped with Eu^{2+}, they have measured light yields in the range 80 000-100 000 photons/MeV and energy resolution of 2-4% at 662 keV [32]-[37]. Growing large single crystals without compromising these excellent metrics is often a challenging and difficult task. In order to understand their properties we have performed detailed studies of the structural and electronic properties of ternary hosts KSr_2I_5, KBa_2I_5, $CsSr_2I_5$, and $CsBa_2I_5$. These have been reported elsewhere [38], [39]. Computational results indicate a

This article has been accepted for publication in a future issue of this journal, but has not been fully edited. Content may change prior to final publication. Citation information: DOI 10.1109/TNS.2016.2632064, IEEE Transactions on Nuclear Science

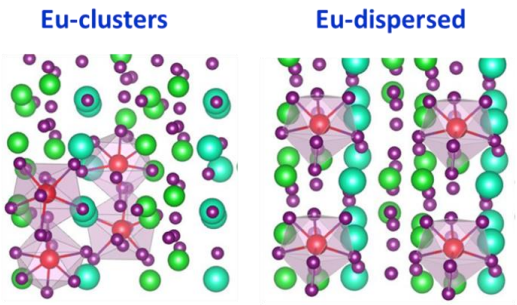

Fig. 4. Schematic plot of possible Eu-rich clusters in Ba-containing compounds. Since Eu prefers B^{VII} site, Eu-clusters are favorable in Ba-containing compounds (left) while Eu-dispersed may be expected in Sr-containing ternaries (right).

TABLE II
RELATIVE STABILITY (ΔE) OF Eu DOPING AT A B^{VII} SITE WITH RESPECT TO B^{VIII}. THE GAP BETWEEN THE Eu $4f^7$ AND THE CBM ($4f$-CBM) WHEN Eu SUBSTITUTES AT A B^{VIII} OR B^{VII} SITE ARE ALSO INCLUDED.

	ΔE (meV)	B^{VIII} $4f$-CBM (eV)	B^{VII} $4f$-CBM (eV)
KSr_2I_5	−19	2.49	2.26
KBa_2I_5	−198	2.51	2.29
$CsSr_2I_5$	−21	2.46	2.36
$CsBa_2I_5$	−143	2.81	2.49

mixed-cation quaternary of the type $A(Ba,Sr)I_5$ may offer better crystal homogeneity and favorable electronic properties. The interest towards (Ba,Sr)-mixed crystals is a direct consequence of Eu^{2+} activator's site preference in these compounds. There are two sites suitable for Eu^{2+} substitution in the AB_2I_5 crystals – a 8-fold coordinated (B^{VIII}) or a 7-fold coordinated (B^{VII}) site. We performed structural optimizations and total energy calculations for the relative stability of Eu at B^{VIII} and B^{VII}, respectively. The calculated relative stability, $\Delta E = E(Eu@B^{VII}) - E(Eu@B^{VIII})$ of Eu doping at the two sites in the AB_2I_5 crystals is shown in Table II. Negative sign of ΔE implies that the Eu prefer the B^{VII} sites. The energy differences, ΔE of the Sr-containing crystals are low (~ −20 meV), implying no particular site preference for the substitutional Eu dopant. However, in the Ba-containing crystals the Eu strongly prefer the B^{VII} sites, having large ΔE magnitude. As a consequence, Eu will occupy *both* B^{VIII} and B^{VII} sites in the Sr-containing ternary crystals, while preferring *only* the B^{VII} in the Ba-containing ternaries. This remarkably distinct Eu-dopant behavior in the two sets of compounds may influence their performance. In Sr-containing crystals we could have two inequivalent but spectrally close Eu^{2+} emission centers arising from the B^{VIII} and B^{VII} sites, which may increase the overlap between the excitation and emissions bands and possibly add to the self-absorption. In Ba-containing crystals, not only does Eu^{2+} prefer B^{VII} sites, they also tend to cluster forming small domains as depicted schematically in Fig. 4. Possibility of Eu-clusters and associated narrowing of the $4f$-CBM gap could damage the electronic and mechanical properties caused by this inhomogeneity, especially in large sized crystals. These implications have been discussed in [38], [39].

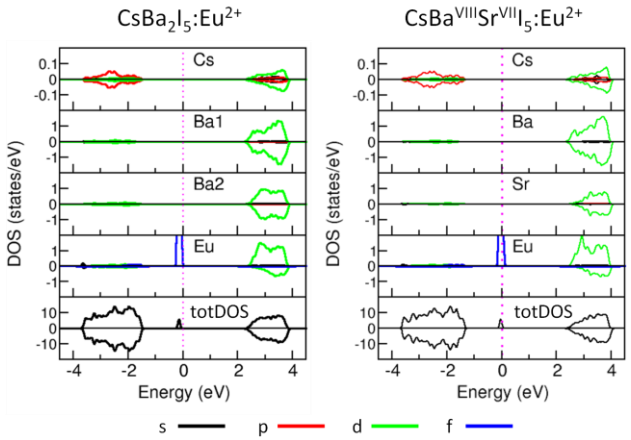

Fig. 5. Total and partial density of states of the metal atoms in $CsBa_2I_5:Eu^{2+}$ and $CsBa^{VIII}Sr^{VII}I_5:Eu^{2+}$ using a 128-atom supercell and PBE+U approach. The Eu $4f^7$ states appear inside the host band gap which is set as the zero of energy.

The above observation about preferential site occupation opens up the possibility of a mixed cation approach, such as $A(Ba,Sr)I_5$. In such a mixed compound we have shown that Ba occupies the 8-fold coordinated B^{VIII} and Sr occupies the 7-fold coordinated B^{VII} sites [38], [39]. Their electronic properties remain similar to the ternaries. Since the substitutional dopant Eu at B^{VII} site is energetically more stable, it is not surprising that in the mixed quaternaries Eu prefers the substitutional Sr site. Our calculations indeed show that Eu substitutes at a Sr site giving $ABa^{VIII}Sr^{VII}I_5:Eu^{2+}@^{VII}$. Fig. 5 shows the electronic DOS of $CsBa_2I_5:Eu^{2+}$ and $Cs(BaSr)I_5:Eu^{2+}$. The valence bands of both host materials appear approximately between -1.5 to -3.8 eV. These states are primarily derived from I 5p and are responsible for trapping and generating STHs. The bottom of the host conduction bands are derived from alkaline-earth d states. The half-occupied Eu $4f^7$ levels appear within the gap of both compounds, while its $5d$ states are resonant with the host CBM. These features, i.e., the proper placement of Eu $4f^7$ inside the gap and $5d$ in the CBM are crucial so that an excited electron may localize at Eu-d, assuming a $4f^6 5d^1$ configuration, ultimately enabling $5d$-$4f$ emission. Fig. 5 reveals no apparent distinction between the ternary and mixed quaternary and we may infer similar, if not identical electronic properties. However, differences in the microstructure are possible within $CsBa_2I_5:Eu^{2+}$ where small, Eu-rich clusters (Fig. 4) will affect the local lattice and alter the electronic and mechanical properties of the crystal. Larger clusters at higher Eu concentrations will exacerbate self-absorption and deteriorate time response of the scintillator [38]. Increase in decay time with increasing Eu concentration has been reported in $CsBa_2I_5:Eu^{2+}$ [35], [37]. There are also indications of crystal inhomogeneity and probable Ba-rich and Eu, Cs-poor phases in $CsBa_2I_5:Eu^{2+}$ [40]. We predict that a mixed cation approach, where the dopant ions are confined to one crystallographic site will lead to uniform doping, allowing more control over Eu concentration, and without the possibility of clustering or crystal inhomogeneity. It also offers a single scintillation center

TABLE III
LATTICE CONSTANTS AND BAND GAP ESTIMATES OF SIX ns^2 COMPOUNDS BASED UPON DENSITY FUNCTIONAL CALCULATION INCLUDING SPIN-ORBIT COUPLING.
THE BAND GAP OF $CsBa_2I_5$ IS SHOWN FOR COMPARISON.

Compound	Lattice constants (Å)			Calculated E_g (eV)
	a	b	c	
$GaSr_2I_5$	10.07	9.16	14.25	4.69
$GaBa_2I_5$	10.57	9.42	14.52	4.77
$InSr_2I_5$	10.03	9.19	14.47	4.53
	(9.98	8.92	14.25)[i]	
	(9.99	8.92	14.26)[j]	
$InBa_2I_5$	10.48	9.49	14.92	4.64
$TlSr_2I_5$	10.00	9.18	14.54	4.44
	(9.97	8.94	14.25)[j]	
$TlBa_2I_5$	10.43	9.31	15.11	4.40
$CsBa_2I_5$	10.75	9.46	15.13	5.15
	(10.54	9.26	14.64)[i]	(5.1~5.5)[l]
	(10.62	9.30	14.70)[k]	

[i]Experimental lattice parameters [30]
[j]Experimental lattice parameters [31]
[k]Experimental lattice parameters [28]
[l]Experimental band gap [37]

eliminating the prospect of inhomogeneous light output from two inequivalent sites. Recent experiments following a similar mixed cation approach were able to grow larger 1.5 cm^3 crystals of $KSr_{1.3}Ba_{0.7}I_5:Eu^{2+}$ with a measured energy resolution of 2.48% at 662 keV [41].

C. *Monoclinic AB_2I_5 compounds containing ns^2 ions*

Our quest in to ternary halides also resulted in a closely related set of compounds where the alkali metal "A" is replaced by ns^2 ions such as Ga, In or Tl (hereafter referred as ns^2 compounds). From a crystal chemistry and electronic structure perspective they are similar to the K or Cs based scintillators such as $CsBa_2I_5:Eu^{2+}$ or $KSr_2I_5:Eu^{2+}$. Our calculations show that these new compounds have a stable monoclinic structure similar to the AB_2I_5 compounds discussed in the previous section. A few of the ns^2 compounds have been experimentally reported as indicated in Table III. The calculated lattice constants are in good agreement with the available experimental values. Although a degree of covalency is introduced by the ns^2 ions, ionic size effects still play a predominant role in determining the bonding environments.

Our first principles based calculations show a modest decrease in band gap compared to $CsBa_2I_5$ (Table III). Unlike $CsBa_2I_5$, we find that the In or Ga antibonding *s* states appear near the valence band maximum (VBM) of the respective compounds (Fig. 6). The Tl *s* states appear slightly below the VBM in $TlBa_2I_5$. The ns^2 ion *p* states dominate near the CBM. In $TlBa_2I_5$, the *p* level forms a narrow spin-orbit split CBM. The consequence of these distinctions among the ns^2 compounds becomes apparent when we attempt Eu doping. Availability of the ns^2 *p* states near CBM will cause an excited electron to occupy those states instead of Eu 5*d* levels that lie higher in the conduction bands, rendering the Eu-dopant ineffective as an activator in these compounds. The scenario is depicted in Fig. 7 where constrained density functional calculations compare the

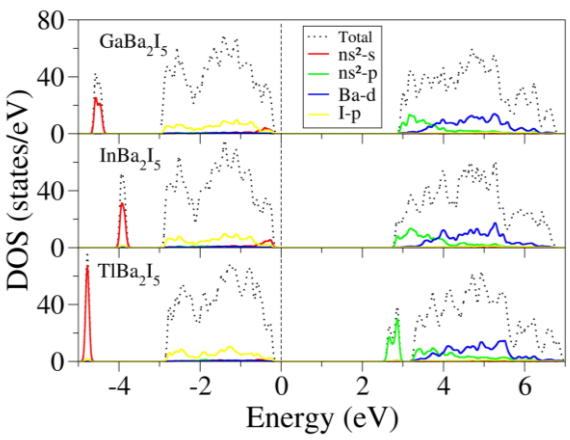

Fig. 6. Total and projected density of states of the ternary ns^2 compounds obtained from PBE-SOC calculations. Note that Ga and In antibonding *s* states appear near the VBM. The ns^2 *p* states (green) dominate near the bottom of the conduction bands. Tl 6*p* forms a spin-orbit split isolated peak at CBM. The zero of energy is set at the top of the valence bands.

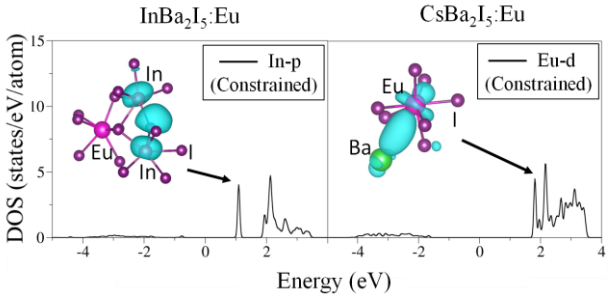

Fig. 7. Projected density of states near the bottom of the conduction bands obtained from constrained excited calculations of Eu-doped $InBa_2I_5$ and $CsBa_2I_5$ (128 atom supercell). The charge density isosurface (0.001 *e*/bohr^3) in $InBa_2I_5$:Eu shows localized electron on In 5*p*, while in $CsBa_2I_5$:Eu the localized electron has a predominant Eu 5*d* character.

electron trapping behavior between $CsBa_2I_5:Eu^{2+}$ and $InBa_2I_5:Eu^{2+}$. Assuming a Eu^{2+}:*($4f^6$) configuration, the excited electron localize on In-*p* creating a polaronic level that descends inside the band gap of $InBa_2I_5$. It is qualitatively different from the constrained calculations of $CsBa_2I_5:Eu^{2+}$ where the excited electron indeed localizes on Eu 5*d*, and 5*d*-4*f* emission becomes possible. This finding about ineffective Eu activation among the ns^2 compounds does not necessarily mean they are nonscintillators. In fact, the differences in the make-up of their VBM and CBM could lead to efficient electron and hole localization and formation of self-trapped excitons (STE). We have recently discussed about the possibility of self-activated scintillation among the ns^2 compounds instigated by In , Ga, or Tl [42]. The critical role of intrinsic STEs in the self-activation of Cs_2HfCl_6 - another ternary scintillator, has been recently highlighted as well in [43], [44].

D. *Orthorhombic ABI_3 ternary halides (A=alkali, B=alkali-earth metal)*

ABI_3 is another family of ternary compounds having promising scintillation properties when doped with Eu^{2+}. Together with the chloride and bromide counterparts, they are drawing attention as materials having light yield and energy

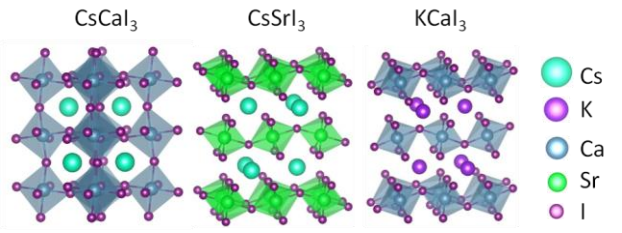

Fig. 8. The crystal structures of orthorhombic $CsCaI_3$, $CsSrI_3$ and $KCaI_3$. $CsCaI_3$ is in Pnma structure while $CsSrI_3$ and $KCaI_3$ are in CmCm. structure.

TABLE IV
THE LATTICE PARAMETERS OF $CsCaI_3$, $CsSrI_3$ AND $KCaI_3$

Compounds	Lattice constants (Å)		
	a	b	c
[i]$CsCaI_3$	8.6226	12.2823	8.5548
[i]$CsSrI_3$	4.8151	15.7842	12.3778
[j]$KCaI_3$	4.561	15.086	11.639

[i]Experimental lattice parameters [31]
[j]Experimental lattice parameters [53]

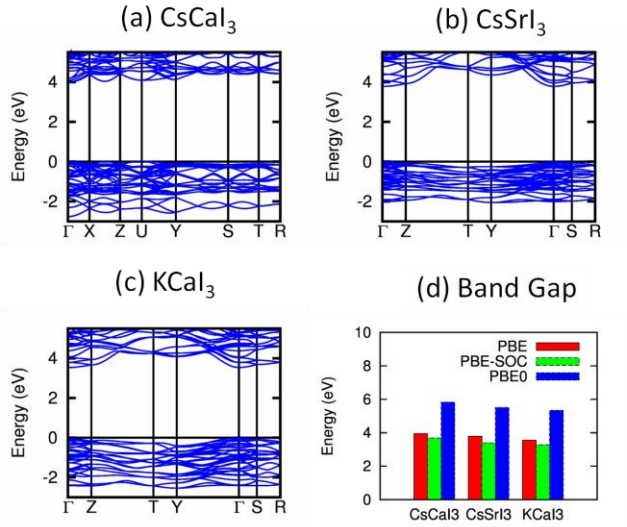

Fig. 9. The band structures of (a) $CsCaI_3$, (b) $CsSrI_3$ and (c) $KCaI_3$ calculated within PBE. The band gap statistics (d) of $CsCaI_3$, $CsSrI_3$ and $KCaI_3$ obtained from PBE, PBE-SOC and PBE0 functionals. The maximum of valence band has been set as zero of energy.

resolution superior to conventional NaI or CsI based scintillators [45-54]. As ternary halides, both ABI_3 and AB_2I_5 have the same constituent binaries AI and BI_2 that are usually good scintillator hosts [55]. Under ambient conditions the ABI_3 compounds stabilize in the orthorhombic or distorted monoclinic structure [31, 47] having larger band gap than the cubic phase which makes them suitable as scintillator hosts.

With an endeavor towards targeted search of new scintillator hosts, we have investigated the electronic structure properties of $CsCaI_3$, $KCaI_3$ and $CsSrI_3$ using *ab-initio* DFT calculations. In [45], reported light yield of $CsCaI_3$ is 38 500 photons/MeV when doped with 3% Eu. An even higher light yield of 51 000 photons/MeV was measured in [50] with reduced resolution of 16.3% at 662keV. For $KCaI_3$ a high light yield of 72 000 photons/MeV and an energy resolution of 3% at 662keV has been reported [53].

At room temperature they all have an orthorhombic structure type, with $CsCaI_3$ belonging to Pnma space group (No. 62) [31] and the latter two belonging to CmCm space group (No. 63) [31], [53]. The structures for the three compounds are shown in Fig. 8. The A cation is at Wyckoff 4c site and B cation takes the 4a position. There are two inequivalent iodines denoted as I1 and I2, respectively. I1 is coordinated with three alkali ions while I2 with two. Both I1 and I2 are coordinated with two neighboring Ca or Sr sites. The experimental lattice parameters used in our calculations are listed in Table IV.

Fig. 9 shows the calculated band structures and energy gaps in $CsCaI_3$, $CsSrI_3$, and $KCaI_3$. They all have wide band gaps around 3.95, 3.79, and 3.56 eV, respectively as obtained from our PBE calculations. Our computed band gap for $CsCaI_3$ is consistent with the calculated value of 4.02 eV in [45, 49], although these values are likely underestimated. One should note $CsCaI_3$ has an indirect gap with CBM at Γ and VBM at U symmetry point of the Brillouin zone, while $CsSrI_3$ and $KCaI_3$ have direct gaps at Γ. The predicted gaps from PBE and PBE-SOC are underestimated due to the well-known shortcomings of semilocal PBE functional. Fig. 9(d) summarizes band gap values of the three compounds calculated with PBE, PBE-SOC and hybrid-PBE0 functionals. Incorporating SOC reduces the gaps by approximately 0.3-0.4 eV compared to PBE values. The PBE0 functional which introduces 25% exact Fock exchange consistently widens the forbidden gap by about 1.7-1.9 eV and are expected to be more accurate predictions. Fig. 9 also shows relatively flat and dispersion-less VBM, a signature in many halides that enables the quick capture of generated holes, forming STHs.

Fig. 10 shows the projected electronic DOS of Eu-doped $CsCaI_3$ obtained from PBE+U calculations. The dopant ion substitutes at Ca cation site due to similarities in valency and ionic radius [56]. In all cases ($CsSrI_3$ and $KCaI_3$ having similar DOSs are not shown), the top of the host valence bands are derived from I 5*p* orbitals and the conduction band edges have a predominant Ca or Sr *d* orbital character. The localized and high-spin Eu $4f^7$ reside inside the host band gap of all three compounds and are well-shielded by the 5*s* and 5*p* electrons. They have antiferromagnetic ordering. The Eu 5*d* orbitals hybridize with the conduction bands. One can observe the similarity between the Eu states shown in Fig. 10 and those of AB_2I_5 compounds in Fig. 5. Although it may be tempting to estimate the optical absorption energy from the energy gap between the highest occupied Eu $4f^7$ and the bottom of the conduction band as shown in Fig. 10, it is worthwhile to mention that the PBE+U method is more suitable for ground state properties, failing to adequately describe excited state behavior. The calculated Eu 4*f*-CBM gap of 2.38 eV is smaller than the lowest experimental absorption and emission energy given in [45] as 2.883 eV and 2.695 eV, respectively. Methods based upon higher level theory and proper accounting of

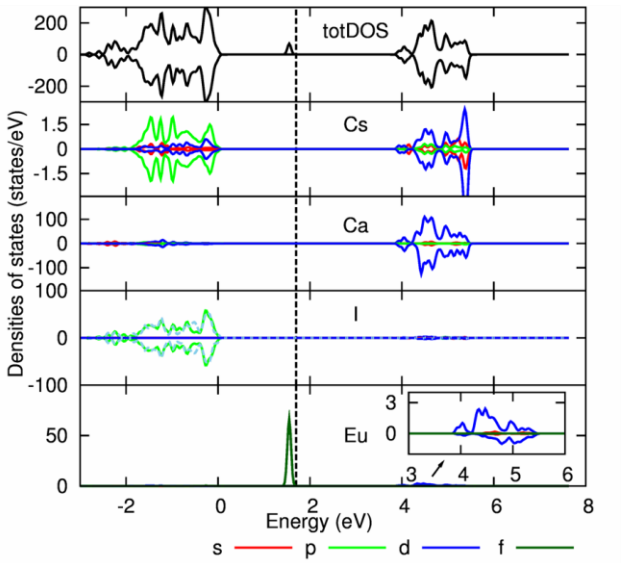

Fig. 10. Projected density of states of $CsCaI_3:Eu^{2+}$ obtained with PBE+*U* calculations. The vertical dashed line shows the highest occupied state, i.e., Eu 4*f*^{7}.

excitonic structures, lattice relaxation of excited system will be able to resolve this discrepancy. In any case, the calculations show the necessary conditions for observed luminescence attributed to Eu^{2+} emission will be fulfilled in these materials; via hole capture at Eu 4*f*, electron capture at Eu 5*d* forming an excited structure followed by 5*d*-4*f* transition. Further work on the excited state behavior, where Eu 5*d* descends inside the band gap, will be helpful to understand quenching effects and trends in this group of compounds.

IV. Conclusion

This work provides a snapshot of our current computational efforts in the area of mixed and stoichiometric "complex" halides that have the potential to surpass NaI or CsI based scintillators. Desirable changes may be possible among the mixed crystals due to changes in the LO phonon frequencies of the intermediate compositions which will impact electron-phonon coupling. While there are changes in the phonon spectrum, electronic properties at the band edges tend to retain the characteristics of the binary end members. It will ensure free carrier-like behavior of the thermalized electron finding its way to a self-trapped hole and eventual radiative recombination. In case of the ternary compounds, we again find favorable characteristics in the electronic structure that support carrier capture and Eu^{2+} activated emission. However, inhomogeneous distribution and Eu-clusters are possible among the Ba-containing $AB_2I_5:Eu^{2+}$ compounds due to preferential site occupation of the dopant ions. In order to circumvent this possibility, our calculations predict (Sr,Ba)-mixed compounds. The ABI_3 set of compounds are also attractive as scintillator hosts due to their favorable band gaps, allowing Eu^{2+} activation. Finally, the ns^2 compounds belonging to the AB_2I_5 group may be interesting as self-activated scintillators. Here, Eu^{2+} doping is rendered ineffective due to lowering of the conduction band edge caused by ns^2 ion *p* states.

Acknowledgment

This material is based upon work supported by the U.S. Department of Homeland Security under Grant Award Number, 2014-DN-077-ARI075-03. This research used resources of the National Energy Research Scientific Computing Center, which is supported by the Office of Science of the U.S. Department of Energy under Contract No. DE-AC02-05CH11231. Computational resources at Arkansas State are partially funded from NSF Grant No. ECCS-1348341.

References

[1] N. L. Cherepy, G. Hull, A. D. Drobshoff, S. A. Payne, E. V. D. van Loef, C. M. Wilson, K. S. Shah, U. N. Roy, A. Burger, L. A. Boatner, et al. "Strontium and barium iodide high light yield scintillators," *Appl. Phys. Lett.*, vol. 92, pp. 083508(1)-083508(3), 2008.

[2] E. V. D. van Loef, P. Dorenbos, C. W. E. van Eijk, K. W. Krämer, and H. U. Güdel, "High-energy-resolution scintillator: Ce^{3+} activated $LaBr_3$," *Appl. Phys. Lett.*, vol. 79, pp. 1573-1575, 2001.

[3] C. Reber, H. U. Guedel, G. Meyer, T. Schleid, and C. A. Daul, "Optical spectroscopic and structural properties of V^{3+}-doped fluoride, chloride, and bromide elpasolite lattices," *Inorg. Chem.*, vol. 23, pp. 3249-3258, 1989.

[4] C. M. Combes, P. Dorenbos, C. W. E. van Eijk, K. W. Krämer, and H. U. Güdel, "Optical and scintillation properties of pure and Ce^{3+}doped Cs_2LiYCl_6 and $Li_3YCl_6:Ce^{3+}$ crystals," *J. Lumin.*, vol. 82, pp. 299-305, 1999.

[5] E. V. D. van Loef, P. Dorenbos, C. W. E. van Eijk, K. W. Krämer, and H. U. Güdel, "Scintillation and spectroscopy of the pure and Ce^{3+} doped elpasolites: Cs_2LiYX_6 (X = Cl, Br)," *J. Phys.: Condens. Matter*, vol. 14, pp. 8481-8486, 2002.

[6] J. Glodo, W. M. Higgins, E. V. D. van Loef, and K. S. Shah, "Cs_2LiYCl_6:Ce Scintillator for nuclear monitoring applications," *IEEE Trans. Nucl. Sci.*, vol. 56, pp. 1257-1261, 2009.

[7] W. M. Higgins, J. Glodo, U. Shirwadkar, A. Churilov, E. V. D. Van Loef, R. Hawrami, G. Ciampi, C. Hines, and K. S. Shah, "Bridgman growth of

Cs_2LiYCl_6:Ce and ^{6}Li-enriched $Cs_2{}^6LiYCl_6$:Ce crystals for high resolution gamma ray and neutron spectrometers," *J. Cryst. Growth*, vol. 312, pp. 1216-1220, 2010.

[8] J. Glodo, E. V. D. van Loef, R. Hawrami, W. M. Higgins, A. Churilov, U. Shirwadkar, and K. S. Shah, "Selected properties of Cs_2LiYCl_6, $Cs_2LiLaCl_6$, and $Cs_2LiLaBr_6$ scintillators," *IEEE Trans. Nucl. Sci.*, vol. 58, pp. 333-338, 2011.

[9] J. Glodo, R. Hawrami, and K. S. Shah, "Development of Cs_2LiYCl_6 scintillator," *J. Cryst. Growth*, vol. 379, pp. 73-78, 2013.

[10] Y. Wu, H. Shi, B. C. Chakoumakos, M. Zhuravleva, M. -H. Du and C. L. Melcher, "Crystal structure, electronic structure, temperature-dependent optical and scintillation properties of $CsCe_2Br_7$" *J. Mater. Chem. C*, vol. 3, pp. 11366-11376, 2015.

[11] E. D. Bourret-Courchesne, G. Bizarri, S. M. Hanrahan, G. Gundiah, Z. Yan, and S. E. Derenzo, "BaBrI:Eu^{2+}, a new bright scintillator," *Nucl. Instrum. Methods Phys. Res., Sect. A*, vol. 613, pp. 95-97, 2010.

[12] R. O. Jones, "Density Functional theory: its origins, rise to prominence, and future," *Rev. Mod. Phys.,* vol. 87, pp 897-923, 2015.

[13] A. D. Becke, "A new mixing of Hartree-fock and local density-functional theories," *J. Chem. Phys,.* vol. 98, pp 1372-1377, 1993.

[14] J. P. Perdew, M. Ernzerhof, and K. Burke, "Rationale for mixing exact exchange with density functional approximations," J. Chem. Phys., vol. 105, pp. 9982 − 9985, 1996.

[15] L. Hedin, "New method for calculating the one-particle Green's function with application to the electron-gas problem," *Phys. Rev.,* vol. 139, pp A796-A823, 1965.

[16] G. Kresse and J. Hafner, "Ab initio molecular-dynamics simulation of the liquid-metal–amorphous-semiconductor transition in germanium," *Phys. Rev. B*, vol. 49, pp. 14251-14269, 1994.

[17] G. Kresse and J. Furthmller, "Efficiency of ab-initio total energy calculations for metals and semiconductors using a plane-wave basis set," *Comput. Mater. Sci.*, vol. 6, pp. 15-50, 1996.

[18] J. P. Perdew, K. Burke, and M. Ernzerhof, "Generalized gradient approximation made simple," *Phys. Rev. Lett.*, vol. 77, pp. 3865-3868, 1996.

[19] P. E. Blöchl, "Projector augmented-wave method," *Phys. Rev. B*, vol. 50, pp. 17953-17979, 1994.

[20] G. Kresse and J. Joubert, "From ultrasoft pseudopotentials to the projector augmented-wave method," *Phys. Rev. B*, vol. 59, pp. 1758-1775, 1999.

[21] A. Zunger, S. -H. Wei, L. G. Ferreira, and J. E. Bernard, "Special quasirandom structures," *Phys. Rev. Lett.*, vol. 65, pp. 353-356, 1990.

[22] S. -H. Wei, L. G. Ferreira, J. E. Bernard, and A. Zunger, "Electronic properties of random alloys: Special quasirandom structures," *Phys. Rev. B*, vol. 42, pp. 9622-9649, 1990.

[23] Y. Wang, J. J. Wang, W. Y. Wang, Z. G. Mei, S. L. Shang, L. Q. Chen, and Z. K. Liu, "A mixed-space approach to first-principles calculations of phonon frequencies for polar materials," *J. Phys. Condens. Matter*, vol. 22, pp. 202201(1)-202201(5), 2010.

[24] S. L. Dudarev, G. A. Botton, S. Y. Savrasov, C. J. Humphreys, and A. P. Sutton, "Electron-energy-loss spectra and the structural stability of nickel oxide: an LSDA+U study," *Phys. Rev. B*, vol. 57, pp. 1505-1509, 1998.

[25] A. Chaudhry, R. Boutchko, S. Chourou, G. Zhang, N. GrønbechJensen and A. Canning, "First-principles study of luminescence in Eu^{2+}-doped inorganic scintillators," *Phys. Rev. B*, vol. 89, pp. 155105(1)-155105(9), 2014.

[26] A. V. Gektin, A. N. Belsky, and A. N. Vesil'ev, "Scintillation efficiency improvement by mixed crystal use," *IEEE Trans. Nucl. Sci.*, vol. 61, pp. 262-270, 2014.

[27] Q. Li, R. T. Williams, A. Burger, R. Adhikari, and K. Biswas, "Search for Improved-Performance Scintillator Candidates among the Electronic Structures of Mixed Halides," *Proc. SPIE,* vol. 9213, pp. 92130M-1, 2014.

[28] D. B. Sirdeshmukh, L. Sirdeshmukh, and K. G. Subhadra, "Alkali halides: a handbook of physical properties," Berlin Heidelberg, Springer-Verlag, 2001, pp. 70-71.

[29] K. Biswas and M. H. Du, "Energy transport and scintillation of cerium-doped elpasolite Cs_2LiYCl_6: Hybrid density functional calculations," *Phys. Rev. B*, vol. 86, pp. 014102(1)-014102(7), 2012.

[30] H. P. Beck, G. Clicqué, and H. Nau, "A study on AB_2X_5 compounds (A: K, In, Tl; B: Sr, Sn, Pb; X: Cl, Br, I)," *Z. Anorg. Allg. Chem.*, vol. 536, pp. 35-44, 1986.

[31] G. Schilling, G. Meyer, "Ternäre bromide und iodide zweiwertiger lanthanide und ihre erdalkali-analoga vom typ AMX_3 und AM_2X_5," *Z. Anorg. Allg. Chem.*, vol. 622, pp. 759-765, 1996.

[32] L. Stand, M. Zhuravleva, A. Lindsey, and C. L. Melcher, "Growth and characterization of potassium strontium iodide: A new high light yield scintillator with 2.4% energy resolution," *Nucl. Instrum. Methods Phys. Res. Sect. A*, vol. 780, pp. 40-44, 2015.

[33] E. D. Bourret-Courchesne, G. Bizarri, R. Borade, Z. Yan, S.M. Hanrahan, G. Gundiah, A. Chaudhry, A. Canning, and S. E. Derenzo, "Eu^{2+}-doped Ba_2CsI_5, a new high-performance scintillator," *Nucl. Instrum. Methods Phys. Res., Sect. A*, vol. 612, pp. 138-142, 2009.

[34] G. Bizarri, E. D. Bourret-Courchesne, Z. W. Yan, and S. E. Derenzo, "Scintillation and optical properties of BaBrI:Eu^{2+} and $CsBa_2I_5$:Eu^{2+}," *IEEE Trans. Nucl. Sci.*, vol. 58, pp. 3403-3410, 2011.

[35] U. Shirwadkar, R. Hawrami, J. Glodo, E. V. D. van Loef, and K. S. Shah, "Promising alkaline earth halide scintillators for gamma-ray spectroscopy," *IEEE Trans. Nucl. Sci.*, vol. 60, pp. 1011-1015, 2013.

[36] M. Gascón, E. C. Samulon, G. Gundiah, Z. Yan, I. V. Khodyuk, S. E. Derenzo, G. A. Bizarri, and E. D. Bourret-Courchesne, "Scintillation properties of $CsBa_2I_5$ activated with monovalent ions Tl^+, Na^+ and In^+," *J. Lumin.*, vol. 156, pp. 63-68, 2014.

[37] M. S. Alekhin, D. A. Biner, K. W. Krämer, and P. Dorenbos, "Optical and scintillation properties of $CsBa_2I_5$:Eu^{2+}," *J. Lumin.*, vol. 145, pp. 723-728, 2014.

[38] C. M. Fang and K. Biswas, "Preferential Eu site occupation and its consequences in the ternary luminescent halides AB_2I_5:Eu^{2+} (A=Li–Cs; B=Sr, Ba)," *Phys. Rev. Applied*, vol. 4, pp. 014012(1)-014012(8), 2015.

[39] C. M. Fang and K. Biswas, "Quaternary Iodides A(BaSr)I5:Eu^{2+} (A = K, Cs) as Scintillators for Radiation Detection," *J. Phys. Chem. C*, vol. 120, pp. 1225−1236, 2016.

[40] S. Lam, S. Swider, J. Fiala, A. Datta, S. "Motakef Microscale luminescence imaging of defects, inhomogeneities, and secondary phases in halide scintillators," *Nucl. Instrum. Methods Phys. Res., Sect. A*, vol. 784, pp. 23-28, 2015.

[41] C. L. Melcher, E. D. Lukosi, M. R. Rust, T. G. Wulz, and K-M. Lee, "Developing low cost scintillators with excellent energy resolution," presented at Domestic Nuclear Detection Office – Academic Research Initiative 9th Annual Grantees Program Review, Atlanta, GA, USA, July 12-14, 2016.

[42] B. Kang, C. M. Fang, and K. Biswas, "A first-principles based study of ns^2 containing ternary iodides and their possibility of scintillation," J. Phys. D:Appl. Phys., vol. 49, pp. 395103(1)-395103(12), 2016.

[43] A. Burger, E. Rowe, M. Groza, K. M. Figueroa, N. J. Cherepy, P. R. Beck, S. Hunter, S. A. Payne, "Cesium hafnium chloride: a high light yield, non-hygroscopic cubic crystal scintillator for gamma spectroscopy," *Appl. Phys. Lett.*, vol. 107, pp. 143505(1)-143505(3), 2015.

[44] B. Kang and K. Biswas, "Carrier self-trapping and luminescence in intrinsically activated scintillator: cesium hafnium chloride (Cs_2HfCl_6)," *J. Phys. Chem. C*, vol. 120, pp. 12187-12195, 2016.

[45] M. Zhuravleva, B. Blalock, K. Yang, M. Koschan, and C. L. Melcher, "New single crystal scintillators: $CsCaCl_3$:Eu and $CsCaI_3$:Eu," *J. Cryst. Growth*, vol. 352, pp. 115-119, 2012.

[46] E. Beurer, Judith Grimm, P. Gerner, and H. U. Gudel, "Absorption, light emission, and upconversion properties of Tm^{2+}-doped $CsCaI_3$ and $RbCaI_3$," *Inorg. Chem.*, vol. 45, pp 9901-9906, 2006.

[47] K. Yang, M. Zhuravleva, and C. L. Melcher, "Crystal growth and characterization of $CsSr_{1-x}Eu_xI_3$ high light yield Scitillators," *Phys. Status Solidi RRL,* vol. 5, pp 43-45, 2010.

[48] U. Shirwadkar, E.V.D. van Loef, R. Hawrami, S. Mukhopadhyay, J. Glodo, and K. S. Shah, "New promising scintillators for gamma-ray spectroscopy: $Cs(Ba,Sr)(Br,I)_3$," IEEE *Nuclear Science symposium and Medical imaging conference,* 2011. DOI:10.1109/NSSMIC.2011.6154636.

[49] M. Tyagi, M. Zhuravleva, and C. L. Melcher, "Theoretical and experimental characterization of promising new scintillators: Eu^{2+} doped $CsCaCl_3$ and $CsCaI_3$," *J. Appl. Phys.,* vol. 113, pp.203504, 2013.

[50] E. Rowe, E. Tupisyn, B. Wiggins, P. Bhattacharya, L. Matei, M. Groza, V. Buliga, A. Burger, N.J. Cherepy, and S. A. Payne, "Double salts Iodide scintillators: Cesium Barium Iodide, Cesium Calcium Iodide, and Barium Bromine Iodide," *Cryst. Res. Technol.,* vol. 48, pp. 227-235, 2013.

[51] M. Zhuravleva, S. Friedrich, and C. L. Melcher, "The Europium oxidation state in $CsSrI_3$:Eu scintillators measured by X-ray absorption spectroscopy," *Opt. Mater.,* vol. 36, pp 670-674, 2014.

[52] M. Suta and C. Wickleder, "photoluminescence of $CsMI_3$:Eu^{2+} (M=Mg, Ca, and Sr) – a spectroscopic probe on structure distortions," *J. Mater. Chem. C,* vol. 3, pp 5233-5245, 2015.

[53] A. C. Lindsey, M. Zhuravleva, L. Stand, Y. Wu, and C. L. Melcher, "Crystal growth and characterization of europium doped $KCaI_3$, a high light yield scintillator," *Opt. Mater.*, vol. 48, pp. 1-6, 2015.

[54] Y. Wu, Q. Li, B. C. chakoumakos, M. Zhuravleva, A. c. Lindsay, J. A. Johnson II, L. Stand, M. Koschan, C. Melcher, "quaternary Iodide K(Ca, Sr)I_3:Eu^{2+} single-crystal scintillators for radiation detection: crystal structure, electronic structure, and optical and scintillation properties," *Adv. Opt. Mat.*, DOI: 10.1002/adom.201600239.

[55] N. J. Cherepy, S. A. Payne, S. J. Asztalos, G. Hull, J. D.Kuntz, T. Niedermayr, S. Pimputkar, J. J. Roberts, R. D.Sanner, T. M. Tillotson, et al., "Scintillators with potential to supersede lanthanum bromide," *IEEE Trans. Nucl. Sci.*, vol. 56, pp. 873-880, 2009.

[56] R. D. Shannon, "Revised effective ionic radii and systematic studies of interatomic distances in halides and chalcogenides," *Acta Cryst.*, vol. A32, pp. 751-767, 1976.